Published in final edited form as:

J Immunol. 2023 June 01; 210(11): 1804–1814. doi:10.4049/jimmunol.2100946.

APE2 promotes AID-dependent Somatic Hypermutation in primary B cell cultures that is suppressed by APE1

Carol E. Schrader[*], **Travis Williams**[*], **Klaus Pechhold**[*], **Erin K. Linehan**[*], **Daisuke Tsuchimoto**[†], **Yusaku Nakabeppu**[†]

[*]Department of Microbiology and Physiological Systems, Program in Immunology and Microbiology, UMassChan Medical School, Worcester, MA 01655

[†]Department of Immunobiology and Neuroscience, Medical Institute of Bioregulation, Kyushu University, Higashi-ku, Fukuoka 812-8582, Japan

Abstract

Somatic hypermutation (SHM) is necessary for antibody diversification and involves error-prone DNA repair of AID-induced lesions in germinal center (GC) B cells but can also cause genomic instability. GC B-cells express low levels of the DNA repair protein APE1 and high levels of its homolog APE2. Reduced SHM in APE2-deficient mice suggests that APE2 promotes SHM, but these GC B-cells also exhibit reduced proliferation that could impact mutation frequency. Here, we test the hypothesis that APE2 promotes and APE1 suppresses SHM. We show how APE1:APE2 expression changes in primary murine spleen B cells during activation, impacting both SHM and class switch recombination (CSR). High levels of both APE1 and APE2 early after activation promote CSR. However, after 2 days, APE1 levels decrease steadily with each cell division, even with repeated stimulation, while APE2 levels increase with each stimulation. When GC-level APE1:APE2 expression was engineered by reducing APE1 genetically (*apex1+/−*) and over-expressing APE2, bona fide AID-dependent VDJ_{H4}-intron SHM became detectable in primary B-cell cultures. The C-terminus of APE2 that interacts with PCNA promotes SHM and CSR, although its ATR-Chk1-interacting Zf-GRF domain is not required. However, APE2 does not increase mutations unless APE1 is reduced. Although APE1 promotes CSR, it suppresses SHM, suggesting downregulation of APE1 in the GC is required for SHM. Genome-wide expression data compares GC and cultured B cells, and new models depict how APE1 and APE2 expression and protein interactions change during B cell activation and affect the balance between accurate and error-prone repair during CSR and SHM.

Keywords

AID; somatic hypermutation; class switch recombination; error-prone repair; AP Endonuclease

Address correspondence to Dr. Carol E. Schrader, UMassChan Medical School, AS8-1015, 368 Plantation St., Worcester, MA 01655. Phone 508-856-6008, Fax 508-856-5920, carol.schrader@umassmed.edu.

Author Contributions: C.E.S. designed and performed experiments, analyzed data, prepared the figures and wrote the manuscript, T.W., K.P. and E.K.L. performed experiments and analyzed data, and D. T. and Y. N. created the *apex2*-deficient mouse line. The authors declare they have no financial conflicts.

Introduction

Somatic hypermutation (SHM) and antibody class switch recombination (CSR) are both initiated by activation-induced cytidine deaminase (AID) and involve error-prone DNA repair. SHM occurs in germinal center (GC) B cells, and while CSR can occur in activated, cultured B cells and a few B cell lines, SHM does not. We previously reported differential expression of the AP endonuclease (APE) DNA repair proteins, APE1 and APE2, in GC B cells, where APE1 expression is surprisingly low and the homolog APE2 is highly expressed. In the absence of APE2, SHM is reduced ~2-fold in Peyer's patch (PP) GC B cells, suggesting repair of AID lesions by APE2 may be error-prone (1), particularly when APE1 expression is limiting. However, APE2-deficient GC B cells also have reduced proliferation and/or survival (2) that could impact mutation frequency. Here we directly test the hypothesis that APE2 promotes and APE1 suppresses SHM.

Both CSR and SHM are initiated by AID, which converts cytosine to uracil in DNA (dU) (3, 4). While the removal of uracil from DNA is normally accomplished by the highly accurate and efficient base excision repair (BER) and mismatch repair (MMR) pathways, dU repair is error-prone at the immunoglobulin (Ig) locus in proliferating B-lymphocytes, resulting in mutations and DNA double-stranded breaks (DSBs) (5). The DSBs are necessary for CSR, and the mutations promote increased affinity of antibody when coupled with selection mechanisms in germinal centers (GCs) (3, 4, 6, 7). Both processes are essential for maturation of the immune response but are also associated with genomic instability such as mutations, translocations, and tumorogenesis, including diffuse large B cell lymphomas (DLBCLs) that are GC cell-derived (Ramiro, Cell 2004) (8).

During accurate repair in non-mutating cells, dU is excised by uracil DNA glycosylase (UNG), leaving abasic (AP) sites that are recognized by APE. APE makes a single strand break (SSB) with a 3' OH that is usually extended by DNA polymerase β (POLB) to replace the excised nucleotide (9). During SHM, dUs may be replicated over before they can be excised and are read as dT by replicating DNA polymerases, resulting in dC to dT transition mutations (3). Also, some AP sites go unrepaired and encounter replication, leading to the non-templated addition of any base opposite the AP site. However, it is not clear why dUs and AP sites escape accurate repair by the highly efficient enzymes UNG and APE1 and lead instead to mutations.

The mismatch repair (MMR) pathway competes with UNG for repair of U:G mismatches. MMR excises a patch surrounding the mismatch, and re-synthesis during SHM involves error-prone translesion polymerases (TLPs) such as Pol η, Pol ζ and Rev1. The MMR pathway is required for the generation of A:T mutations during SHM, and also generates DBSs in S regions that are necessary for CSR (10–13). The collision of BER and MMR pathways, both of which can repair U:G mismatches, and the use of a 'non-canonical' MMR pathway during G1 phase (14), when AID is active (15) partially explains error-prone repair of AID-induced lesions, contributing to mutations and DNA break formation. However, both MMR and BER are active in cultured B cells that undergo CSR and hypermutation at S regions (11), while SHM of the V genes remains undetectable (16–19).

There are two APE homologues, which we found are differentially expressed in the GC relative to cultured B cells (1). APE1 is the major mammalian AP endonuclease; it is ubiquitously expressed, highly efficient, and essential for early embryonic development in mice and for viability of human cell lines (20–22). APE1 interacts with XRCC1, which coordinates SSB repair via PolB and Ligase (23, 24). In contrast, APE2 is a non-essential homologue with very weak AP endonuclease activity (25, 26). APE2 lacks the N-terminal XRCC1-interacting domain of APE1, instead having a unique C-terminus with a PCNA-interacting domain (27–29). PCNA is known to interact with several proteins that are necessary for SHM including UNG, MMR proteins, and error-prone TLPs (30–34). Expression of APE1 is very low in GCs, where APE2 expression is highly induced (1, 35, 36). In APE2-deficient GC B-cells, both SHM frequency and the spreading of mutations beyond AID hotspots is reduced (1, 37), suggesting that repair pathways using APE2 might be error-prone. In contrast to the GC, activated, cultured B-cells express APE1 and APE2 more equally, and SHM of the V genes does not occur.

Here, we studied APE1 and APE2 expression during B cell activation and asked how perturbation of APE1 and APE2 levels impacts CSR and SHM. To avoid the complication of reduced proliferation and/or survival of APE2-deficient GC B-cells, we developed an in vitro system where APE2-deficient B cells proliferate normally (35), and where we can manipulate the ratio of APE1:APE2 expression levels. We found that APE2 is indeed error-prone, promoting CSR and mutations in the Sμ region. Furthermore, APE2 also promotes AID-dependent SHM in the V region J_{H4} intron in cultured B cells, but only when APE1 levels are reduced. Although APE1 promotes CSR, it suppresses SHM.

Materials and Methods

Mice

All mouse strains were backcrossed to C57BL/6 for more than 8 generations, (except B1-8, 5 generations) and prior to interbreeding to create double-deficient mice. AID-deficient mice were obtained from T. Honjo (Kyoto University, Kyoto, Japan). *Apex1*$^{+/-}$ mice were obtained from E. Friedberg (38) (University of Texas Southwestern Medical Center, Dallas, TX). MSH2-deficient mice were obtained from T. Mak (University of Toronto, Toronto, Canada) and UNG-deficient mice were obtained from T. Lindahl and D. Barnes (London Research Institute, London England). APE2-deficient mice (39) and B1-8 mice (40) were previously described. Because *apex2* is on the X chromosome, we used male *apex2*$^{Y/-}$ mice in all experiments. The WT mice were littermates of either the *apex2*$^{Y/-}$ or *apex1*$^{+/-}$*apex2*$^{Y/-}$ mice. Mice were housed in the Institutional Animal Care and Use Committee (IACUC)-approved specific pathogen-free facility at the University of Massachusetts Medical School. The mice were bred and used according to the guidelines from the University of Massachusetts IACUC.

CSR and SHM primary B cell culture system

B cells were enriched from mechanically dispersed spleen by T-depletion with antibody and complement followed by centrifugation over Lympholyte (Cedar Lane), as previously described (19), and activated with LPS, anti-IgD-dextran, and BLyS-FLAG. IFNγ was

added to cultures for IgG2a CSR. Cells were infected with retrovirus (RV), described below, 24h after activation and cultured for 2 or 4 additional days for CSR and SHM analysis, respectively. Tamoxifen was added to cultures with pMX-PIE RV to force the ER− tagged construct into the nucleus. For GLSμ and J_H4 mutation analysis, four independent cultures for each RV infection were set up to maximize the potential for unique clones and unique mutations. 2 days after infection, cultures were split and fed with fresh medium, tamoxifen and switch inducers to promote viability and continued cell division. Viable cells were isolated by flotation on Lympholyte 4 days after infection, and GFP+IgM− and GFP+IgM+ cells from each culture were sorted independently on a FACSAriaIIu® (Becton Dickson) after staining with anti-IgM-PE (Southern Biotech) and 7AAD. Two or three experiments were performed for each RV analyzed. There was no difference in viability in any of these cultures (Suppl. Fig. 2). SHM was analyzed in IgM^- cells, which have undergone CSR and therefore experienced AID activity, and GLSμ was analyzed in IgM+ cells, which have the μ switch region intact.

Retroviral Constructs

pMX-PIE-AID-FLAG-ER-IRES-GFP-*puro* (41) was received from Drs V. Barretto and M. Nussenzweig (The Rockefeller University, NY). The control retrovirus, pMX-PIE-ER-IRES-GFP, was constructed and viruses were prepared as previously described (42). pMIG (43) was received from Dr J. Chaudhuri (Sloan-Kettering Memorial Cancer Center, NY). Full-length APE1, APE2 and truncation mutants were generated by PCR, cloned into Bluescript (Stratagene), confirmed by sequencing, and subcloned into pMX-PIE and pMIG. To create the APE2 PIP2 substitution mutant, the APE2 gene in Bluescript was mutated using Quik-Change (Stratagene), sequenced, and then reinserted into pMX-PIE and pMIG. Retroviruses were produced in Phoenix-E cells with pCL-Eco and X-tremeGene (Roche).

Western Blotting

Pelleted cells from FACS-purified or cultured B cells were lysed in RIPA buffer, and 15-20 μg of whole cell extracts were analyzed on 8% polyacrylamide gels as described previously (19) with polyclonal goat anti-APE1 (R&D Systems), rabbit anti-APE2 (AnaSpec, (35)), anti-POLB, rabbit anti-Grb2 (growth factor receptor bound protein 2), anti-ER, and anti-GAPDH (glyceraldehyde 3 phosphate dehydrogenase) (SantaCruz) primary antibodies, with goat anti-rabbit and donkey anti-goat secondary antibodies coupled to horseradish peroxidase (SantaCruz).

Amplification, cloning and sequence analysis of GLSμ and J558VHFR3-JH4 3’ intron segments

DNA was prepared from FACS-purified cells by proteinase K and RNaseA digestion and ethanol precipitation. To assay SHM, a 492 bp fragment of the V_HJ558L framework 3 - J_H4-3’ flanking region was amplified by a nested PCR using Pfu Ultra II (Stratagene); primers were modified slightly from (44). Primers for the first amplification were: forward 5’AGCCTGACATCTGAGGAC and reverse 5’ GTGTTCCTTTGAAAGCTGGAC. Nested primers for the second amplification were: forward 5’ CCGGAATTCCTGACATCTGAGGACTCTGC and reverse 5’ GATGCCTTTCTCCCTTGACTC. The reaction conditions for the first primer set were

95°C for 30 seconds, 57° for 30 seconds, and 72° for 1 minute for 30 cycles; and for the second primer set were 95° for 30 seconds, 57° for 30 seconds, and 72° for 1 minute for 35 cycles. PfuTurbo (Agilent) (error rate = 1.3 x 10^{-6}) was used to amplify a 749 bp 5' GL Sμ fragment as described (45). Primers were: 5u3 (forward primer) 5'-AATGGATACCTCAGTGGTTTTTAATGGTGGGTTTA-3' (46) and m2R (reverse primer) 5'-GCTACTCCAGAGTATCTCATTTCAGATC-3' (47).

The PCR products were electrophoresed on 1% agarose gels; the Sμ and JH4 bands were purified using QIAquick Gel Extraction Kit (Qiagen), dA tails were added with Taq polymerase, cloned using TOPO TA cloning kit (Invitrogen), and sequenced by Macrogen (Boston MA). We select only 24 colonies from each of the four independent cultures for a total of 96 clones sequenced from each experiment, to avoid repeat CDR3s. Unmutated sequences were not excluded from mutation frequency calculations.

Flow Cytometry and FACS-purification of GC and cultured B cells

Peyer Patches were excised from 12-20-week-old, naive, WT mice, mechanically dispersed on ice and passed through 45 um nylon mesh. For intracellular APE1 analysis, PP or cultured B cells were stained with Live/Dead Blue (Thermo Fisher) (1:200) in PBS, washed and surface stained with B220 VioGreen (1:50), GL7 FITC (1:300), CD95 PE (1:50), CD86 PE-Cy7 (1:100), and CXCR4 Per-CP-EF710 (1:50) then washed with PBS, fixed with 2% formaldehyde and permeabilized with 0.1% saponin buffer prior to staining with goat IgG anti-APE1 (R&D Systems) (1:120) in saponin buffer, then donkey anti-goat Dylight 649 (1:300, Jackson Immunoresearch) in saponin buffer, washing with saponin buffer after each step. Fc Block was added prior to staining. For proliferation studies, cells were stained with CellTrace Violet (Thermo Fisher) prior to culture, and B220 FITC (1:200) prior to APE1 intracellular staining as above. Analysis was done on a 4-laser (R/B/V/YG) Aurora cytometer (Cytek Biosciences). The following antibodies were used for FACS-purification and genomic analysis: REAffinity mAbs CD45R/B220 (REA755, VioGreen), and CD95 (REA453, PE-Vio770) (Miltenyi Biotec), biotinylated GL7 (IgM, BioLegend) followed by SA-APC/Cy7 (BioLegend), and Live-or-Dye NucFix fixable dead cell staining kit (Biotium).

Genomic profiling was achieved using Templated Oligo Sequencing (TempO-Seq®, Biospyder Technologies). Briefly, integrated (optional) intracellular (ic) staining with mRNA in situ hybridization (icTempO-Seq) was carried out on non-sorted cell suspensions after surface staining (optional), dead cell labeling, fixation and permeabilization. Cells (approx. 10^5/sample, in multiples when necessary) were then "ic-stained" using a mouse whole transcriptome array with DNA-oligo (DO)-probe sets (msWT-Assay: 30,146 dual DO sets covering 21,450 distinct mouse gene transcripts) at 0.2 nM in 100 ul/sample Hybridization Solution (Biospyder), supplemented with 0.1% saponin and murine RNase inhibitor (M0314, NE Biolabs), then overlayered with mineral oil and incubated at 45°C overnight. The next day, cells were washed, and DO-probes ligated in situ with Ligation Buffer (Biospyder) for 1h in a H_2O-saturated 37°C CO2-incubator. After another wash, cells were suspended in FACS sample buffer and sorted on a BD FACSAriaII using stringent doublet- and dead cell-exclusion gating. Sorted populations typically in a 4-way sort setup

included: single GC B-cells (B220+, CD95+, GL7+), follicular naïve B-cells (B220+, CD95-neg, GL7-neg), and in vitro cultured B-cells (B220+, CD95+, GL7+) using the same staining and hybridization protocol. All sorted subsets were >95% pure upon reanalysis. 100 cells/sample were accurately adjusted either by plate sorting, in which case a second round of FACS sorting with identical gates was used, or by precisely adjusting FACS-sorted cell concentrations by aliquot counting (MACSQuant Analyzer using volume counting option).

Next Generation Sequencing and statistical analysis of gene profiles.

Sequencing libraries were prepared from FACS-purified cells (100 cells/sample) by one 28-cycle, single-plex barcoding PCR (Index PCR Plates and PCR settings, Biospyder), followed by library pooling and clean-up (NucleoSpin, Machery-Nagel). Libraries were run on NextSeq High Output (~ 450 million reads) or HiSeq (~ 250 million reads/lane) with pooled samples requiring ~ 3 million reads/sample of WT array. Sequences were aligned and statistically analyzed using the TempO-Seq®-R cloud-based software package (Biospyder), applying the DeSeq2 method for differential analysis of RNA-Seq data (48).

Results

APE1 expression in cultured and GC B cells.

APE1 expression previously assessed by western blotting appears very low in the GC relative to activated, cultured B cells, while APE2 is highly expressed in both (1). To better understand the dynamics of APE1 expression, we sought to determine the distribution of expression at the single cell level in both GC and cultured B cells. Since western blotting provides only an average expression level, we developed an intracellular stain to track APE1 by flow cytometry. We first asked whether expression differed between the dark zone (DZ), where rapid proliferation and mutation takes place, and the light zone (LZ), where selection occurs and B cells are in transit, entering and exiting the GC. We found that, compared to activated cultured B cells that express nearly uniform, high levels of APE1 (Fig. 1A (top row), 83% $APE1^{hi}$), GC B cells express varying levels of APE1 and only about 20% are $APE1^{hi}$ (Fig. 1A, middle row). $APE1^{lo}$ GC cells comprise both light zone (LZ) and dark zone (DZ) B cells, whereas $APE1^{hi}$ cells are skewed toward the LZ (Fig. 1A (bottom row) and 1B). Interestingly, $APE1^{hi}$ cells are enriched in CXCR4/CD86 double-positive cells, which we speculate might be in transition (Fig. 1A, bottom right). We conclude that low APE1 expression in the GC correlates with the proliferation and mutation that occurs in the DZ.

We then evaluated regulation of APE1 expression during B cell activation in culture where CSR but not SHM occurs. We found that APE1 RNA and protein levels are both high up to 48 hr post-activation and then begin to decline (Fig. 1C and D). In contrast, APE2 RNA levels are steady throughout the culture. Using cell trace violet to track cell division, we find that APE1 protein levels are stable and independent of cell division at 2 days (48 - 53 hr) post-activation when RNA is high. However, in cells harvested after 2.5 days (~67 hr) in culture, APE1 decreases steadily in proportion to the number of cell divisions (Fig. 1, E, F, G), even though cells were re-stimulated every 2 days to promote proliferation. Thus, there is a time-dependent decrease in expression, consistent with the decrease we see

in mRNA expression, but in addition, the remaining APE1 protein is diluted out by cell division. Biologically, high APE1 expression correlates with CSR activity, which peaks 2 – 3 days after activation, and low APE1 occurs after cells have undergone many rounds of cell division, as in the GC, correlating with SHM. Indeed, after the initial activation phase (24 – 48 hr), the more times a cell divides, the less APE1 is has.

CSR in cultured B cells with altered APE1 and APE2 levels.

We next sought to determine the impact of the dynamic changes in APE expression on SHM and CSR. We developed a culture system where we could manipulate the expression levels of APE1 and APE2 in ex vivo primary spleen B cells both genetically and by retroviral (RV) overexpression. Unlike GC B cells, these cells historically do not undergo SHM but do proliferate normally in the absence of APE2, presumably due to higher APE1 expression. *apex2* is on the X chromosome, so APE2-deficient cells from male $apex2^{Y/-}$ mice were used. Since APE1-deficiency is embryonic lethal, we used $apex1^{+/-}$ mice that are haploinsufficient to reduce APE1 expression (38). To reduce APE as much as possible, we crossed $apex1^{+/-}$ and $apex2^{+/-}$ mice. These mice are haploinsufficient for APE1 *and* APE2-deficient, which we term “DBL” (double: $apex1^{+/-}apex2^{Y/-}$). Splenic B cells were activated with LPS, anti-IgD-dextran, IFN-γ and BLyS, and then infected with retrovirus (RV) to express estrogen receptor (ER)-tagged APE1, APE2 or ER tag alone (Fig. 2), or untagged proteins (Supplementary Fig. 1A, B), all expressed with a bicistronic GFP reporter. Tamoxifen was added during retroviral infection to force the ER-tagged construct into the nucleus. Expression levels of endogenous APE1 and APE2, and RV APE2-ER, are shown in these cultures by western blotting (Fig. 2A).

We first evaluated the effect of perturbed APE1 and APE2 levels on CSR, since we found previously that both APE1 and APE2 contribute to DSB formation in Sμ and to optimal CSR (35). We find here that neither APE1 nor APE2 are limiting for CSR in WT B-cells, as over-expression of neither RV-APE1-ER nor RV-APE2-ER altered CSR to IgG2a (Fig. 2B). As in our previous report, CSR in APE2-deficient B cells ($apex2^{Y/-}$/ER) is reduced to 60% of WT levels (WT/ER) and we now find that CSR is fully restored by expression of RV-APE2 ($apex2^{Y/-}$/APE2, Fig. 2C). In DBL B-cells, CSR is further reduced to only 40% of WT levels (Fig. 2D), where expression of RV-APE2 restores CSR to ~70% of WT CSR. Over-expression of RV-APE1 does not increase CSR in B cells that are deficient for APE2 ($apex2^{Y/-}$ or DBL). The same results were obtained using untagged APE proteins, and for CSR to IgG3 (Supplementary Fig. 1 A, B). These data support our previous conclusion (35) that APE1 and APE2 work together for optimal CSR.

Germline Sμ mutations.

We then asked whether APE1 and APE2 levels impact the AID-dependent mutations that accumulate in GLSμ prior to successful switch recombination. B cells were activated for CSR and infected with RV, but then fed with fresh activators and tamoxifen on day 3 and cultured for an additional 2 days prior to FACS-purification of RV-infected (GFP^+) cells that remained IgM^+, indicating lack of successful CSR. These cells have a high mutation rate at GLSμ (WT/ER, 9.5×10^{-4} mutations/bp) that is AID-dependent. The mutation frequency and number of mutations per sequence are shown in Fig. 2E, Suppl. Fig. 2 and

Supplementary Table 1). B cells with reduced APE1 (*apex1*$^{+/-}$/ER) have a 1.3-fold, highly significant increase in mutations vs. WT/ER, consistent with an accurate repair role for APE1. However, the opposite is observed for APE2, where mutations are reduced by almost half in the absence of APE2 (*apex2*$^{Y/-}$/ER vs. WT/ER) and are restored by expression of RV-APE2 (WT/ER vs. *apex2* $^{Y/-}$/APE2-ER, n.s.). In DBL B cells, mutations are also reduced by half, and again restored by RV-APE2. Note that the increase in mutations seen with reduced APE1 (*apex1*$^{+/-}$/ER) occurs only if APE2 is present, i.e. not in DBL B cells. Surprisingly, when APE1 is over-expressed, the GLSμ mutation frequency increases slightly relative to control (DBL/APE1-ER vs. DBL/ER, $p = 0.02$). However, the increased frequency is due to one highly mutated sequence (Suppl. Fig. 2, DBL/APE1) and includes a high frequency of insertions and deletions (InDels), which can be indicative of DNA breaks (Fig. 2F), consistent with the highly efficient endonuclease activity of APE1. Interestingly, even though there is a 4-fold increase in InDels with DBL/APE1-ER expression, this condition, which lacks APE2, does not promote efficient CSR (Fig. 2D). InDels are also increased in apex1/ER cells, but these cells express endogenous APE2 and CSR is only modestly reduced in *apex1*$^{+/-}$ B cells (≈ 80% of WT) (35). As such, when levels of APE1 and APE2 are perturbed, APE2 expression and the frequency of GLSμ mutations correlate better with efficient CSR than do APE1 expression and InDel mutations, suggesting the InDels may indicate breaks that are processed in a way that does not promote CSR. We conclude from these data that APE1 and APE2 work together to promote efficient CSR and that low-level APE1 expression is sufficient. Furthermore, APE2 contributes significantly to the generation of AID-dependent mutations at GLSμ.

Perturbation of APE levels in cultured B cells promotes SHM.

Our GLSμ analysis suggests that AP site repair by APE2 may be error-prone, in agreement with our findings in PP GCs, where both very low APE1 and high APE2 expression contribute to SHM of V genes (1). In contrast, cultured B cells highly express both APE1 and APE2 (1, 35) and SHM of the V genes does not occur. To test our hypothesis that APE2 actively promotes mutations, we used the same culture system as for GLSμ mutations and examined the impact of altered APE1:APE2 expression levels on V-region mutation frequency.

In *apex1*$^{+/-}$ B cells expressing RV-APE2, the ratio of APE2:APE1 was determined by western blotting as a function of time in culture (Fig. 3A), and after 48 hr is comparable to what we previously observed in GC B cells (1). The arrows below Fig. 3A indicate when fresh stimulators and/or RV are added. RV-APE2 is detectable at constitutively high levels throughout days 2-5 of the culture at much higher levels than endogenous APE2, which is induced upon activation and then decreases, cycling with repeated stimulations on d.0, 1, and 3. *apex1*$^{+/-}$ B cells express about half as much APE1 as WT, and levels decrease slowly and steadily with time in culture, despite repeated stimulation and in agreement with our intracellular stain results for APE1 (see Fig. 1). Interestingly, endogenous POLB also appears to cycle with activation as does APE2. This culture system mimics GC B cells with rapid proliferation, multiple rounds of stimulation, low levels of APE1 and high levels of APE2 expression.

To analyze SHM in vitro, we used DBL B cells so that APE1 is low, and APE2 is deleted and can be replaced with WT or mutated APE2. On day 5 of culture, we purify GFP+IgM− cells, which have undergone CSR and therefore experienced AID activity, and clone and sequence the J_{H4} intronic region that lies 3' to recombined J558VDJ$_{H4}$ genes, the most abundant V gene family in mice. The J_{H4} intronic region is routinely analyzed for SHM in GC cells as it undergoes mutation but is not subject to selection. As previously shown by others, we found no significant difference in mutations between WT and AID-deficient cultured B cells. However, in APE1 haploinsufficient B cells (*apex1*$^{+/-}$/ER) there is a significant, two-fold increase in mutations compared to AID-deficient B cells (aid$^{-/-}$/ER), similar to our results at GLSμ. With added overexpression of RV-APE2 (*apex1*$^{+/-}$/APE2-ER), we see a further increase in mutations that is 2.7-fold higher than aid/ER and 1.9-fold higher than WT/ER (Fig. 3B and Supplementary Table 2). APE2-deficient cells with WT APE1 levels (*apex2*$^{Y/-}$/ER) also have increased mutations (including a rare-occurring InDel) and re-expressing APE2 in these cells (*apex2*$^{Y/-}$/APE2-ER) brings mutations back to WT levels. This suggests that it is not merely APE2 or APE2-ER expression, but rather perturbation of APE1:APE2 levels that promotes SHM. However, decreased APE1 levels do not promote SHM in the absence of APE2 (DBL/ER), whereas mutations in DBL B cells expressing APE2 (ER or un-tagged) are increased 2.4-fold and 1.8-fold, respectively, relative to WT/ER control. The slightly higher mutation rate in DBL/APE2-ER is not significantly different from DBL/APE2-pMIG or *apex1*$^{+/-}$/APE2-ER. Importantly, over-expression of APE2 does not induce J_{H4} mutations in cultured B cells when APE1 is at normal levels (*apex2*$^{Y/-}$/APE2-ER). The mutation frequency in DBL/ER and WT/ER control cultures was similar to *aid*$^{-/-}$/ER B cells, and to that reported for J_{H4} mutations in B1-8 *aid*$^{-/-}$ cultured B cells (0.9 x10^{-4}) (18). Sequences with identical CDR3s are rare (~5%) and omitted from analysis. The unique CDR3s indicate we are not merely expanding clones with prior mutations. To show that perturbed APE levels do not cause random genome-wide mutations, we sequenced a 595 nt segment of *msh6* DNA from DBL/APE2-ER cells, and the mutation frequency was similar to *aid*$^{-/-}$/ER background (Supplementary Table 2).

To further validate that mutations were AID-dependent, we tested *msh2*$^{-/-}$*ung*$^{-/-}$ B cells infected with control RV-ER, where AID-induced dU's will go largely unrepaired and read as C ➔ T or G ➔A transition mutations. The mutation rate in these cells was 4.9 x 10^{-4}, which is 5-fold higher than *aid*$^{-/-}$/ER background and 2-fold higher than in *DBL*/APE2-ER cultures (Supplementary Table 2). Furthermore, 17 out of 18 mutations were G:C to A:T transitions, as expected if mutations are induced by AID. Also, APE2-ER did not promote mutations in DBL B cells in the absence of AID (Suppl. Table 2, see DBL x *aid*$^{-/-}$/APE2-ER). These data show that AID does act on V(D)J genes in cultured B cells, but that the dU's are normally repaired by error-free mechanisms, which we show here to include APE1. Thus, engineering APE levels to resemble those seen in the GC promotes low-level AID-dependent SHM at the J_{H4} intron in cultured primary B cells.

Since the mutation frequency at J_{H4} intron in culture is much lower than occurs in the GC, we asked if SHM would be higher in the VDJ exon by using B cells from B1-8 mice (40). We backcrossed B1-8 mice to C57BL/6 background for 5 generations and then bred B1-8 mice that were MSH2− and UNG-deficient, or *DBL (apex1*$^{+/-}$*apex2*$^{Y/-}$*)*, with or without AID-deficiency. We saw a 3-fold increase in mutations in B1-8/*msh2*$^{-/-}$*ung*$^{-/-}$ mice vs.

B1-8/*aid*$^{-/-}$, all of which were transitions at G:C bp, again indicating AID activity at the V region (Suppl. Table 2). However, this was unexpectedly lower than the mutation frequency we detect at J_{H4} in C57BL/6 and surprisingly, APE2 overexpression had no effect on SHM in DBL (*apex1*$^{+/-}$*apex2*$^{Y/-}$) B1-8 B cells (Suppl. Fig. 3C). Since we showed above that APE2 does not increase mutation frequency unless APE1 is decreased, we examined APE1 expression levels in B1-8 B cells and found that APE1 levels are indeed higher in B1-8 cultured B cells relative to C57BL/6 B cells by western blotting and by flow cytometry (Suppl. Fig. 3A, B, D). Increased APE1 expression is also seen *in vivo* in this widely used mouse model, as shown in PP GC cells (Suppl. Fig. 3E, F). Although we did not observe increased mutation frequency in the VDJ exon as expected, our results in the B1-8 model further demonstrate that APE2 does not increase SHM unless APE1 expression is low.

The APE2 C-terminus contributes to CSR and mutations.

To try to understand how APE2 contributes to SHM, we explored the domains of APE2 that could regulate accuracy of repair. APE1 and APE2 share a core domain that is highly conserved, with the exception of two amino acid changes in the active site that reduce the relative endonuclease activity of APE2 by several orders of magnitude (26). Also, as shown in Fig. 4A, APE1 has a unique N-terminus that interacts with XRCC1 (23, 24), while APE2 has a unique C-terminus with three domains that are conserved between mouse and human: (1) aa 314-364, of unknown function, (2) a functional PCNA-interacting motif (PIP-box; aa 390-397), and (3) a zinc-finger (Zf-GRF) domain (aa 455-516) that interacts with ss DNA and activates ATR/Chk1 to stimulate SSB repair (27–29). To explore whether these domains impact the role of APE2 in CSR and SHM, we made a series of truncation mutants and also mutated two amino acids in the PIP domain that were previously shown to block PCNA interaction with human APE2 (28) (Fig. 4A). All are stably expressed in B cells (Fig. 4B) and do not impact viability (Supplementary Fig. 4). We found that APE2-ΔC, which lacks the entire unique C-terminus, cannot restore CSR in DBL B cells (Fig. 4C). APE2-ΔD, which lacks the PIP and Zf-GRF domains, partially restored CSR (1.4-fold over RV-ER control, $p < 0.005$), while APE2-ΔE, which has the PIP domain but lacks the Zf-GRF domain, fully restores CSR, frequently to a higher level even than full-length APE2. The same results were found in cells expressing the untagged proteins, although APE2-ΔD was even more effective without the C-terminal ER tag and not significantly different than full-length APE2 (Supplementary Fig. 1C). APE2-PIP2, with two key amino acids in the PIP domain mutated, was also able to fully restore CSR (Fig. 4C). Although mutations in the PIP domain did not reduce CSR efficiency, we could not rule out a role for PCNA, because PCNA has been shown to interact functionally with APE2 via the Zf-GRF domain in addition to the PIP box (29). As this domain is intact in APE2-PIP2, this mutant might still interact with PCNA. We conclude that part of the C-terminus is required for the role of APE2 in CSR, but the Zf-GRF domain is not.

GLSμ mutations were lower in all the mutants, although APE2-ΔE-expressing cells had mutation frequencies near that of full-length APE2 (Fig. 4D). Interestingly, APE2-ΔE caused a highly significant increase in InDels (Fig. 4E), similar to that seen in APE1 over-expressing cells (see Fig. 2F). This suggests that the C-terminal ATR-ChK1-interacting domain that is lacking in APE2-ΔE might indeed stimulate SSB repair, thus slightly

suppressing CSR. As DBL/PIP2 cells also had increased InDels, we speculate that this C-terminal mutation might also interfere with ATR-ChK1-interaction.

J_{H4} mutations are differently affected by the APE2 mutants than are CSR and GLSμ mutations. Expression of all APE2 mutants increased J_{H4} mutations relative to ER control, although APE2-ΔC was of borderline significance, $p = 0.06$ (Fig. 4F). APE2-ΔD-expressing cells have the highest frequency of mutations. APE2-ΔD appears the most highly expressed by western in Fig. 4B, however, this could reflect transfection efficiency since mutation and CSR analyses were gated for GFP+ cells, while the extracts for western analysis were made without sorting for GFP+ cells expressing RV. RV-APE1 did not increase J_{H4} mutation frequency. We conclude that, even without the C-terminus, the inefficient endonuclease activity of APE2 promotes mutations in these cultures.

Mutation spectra.

Analysis of the J_{H4} mutations observed is shown in Supplementary Table 2, although the low number of mutations relative to background, random mutations make it difficult to draw conclusions. However, one observation is noteworthy. InDels were detected in J_{H4} only in 3 conditions: APE2-deficiency (apex2$^{Y/-}$/ER), or RV-APE1 or APE2-ΔE over-expression (Supplementary Table 2), similar to what we found in GLSμ. This is consistent with a high APE1:APE2 ratio favoring DNA breaks, and also with the APE2 C-terminal ATR/Chk1 domain that is absent in ΔE stimulating SSB repair in culture. The presence of this domain in WT APE2 presents another example of the balance between accurate and error-prone repair that occurs during CSR and SHM.

Gene expression in GC vs. cultured B cells.

Since the pattern of APE1:APE2 expression differs between GC and cultured B cells and impacts mutation frequency, we performed whole transcriptome profiling on both populations to gain further insight into the gene expression context of in vitro stimulated B-cells exhibiting a low mutation frequency. Genomic profiling was achieved using Templated Oligo Sequencing (TempO-Seq®, Biospyder Technologies) (49), a modified version of RNA Annealing, Selection, and Ligation with massive parallel sequencing (RASL-Seq) adapted for FFPE samples (50–52), and further adapted to permit intracellular staining prior to FACS-purification of B-cell subsets. Of 21,450 genes surveyed, 11,780 were detected, of which 1,711 (14.5%) were significantly down- and 3,219 (27.3%) up-regulated (adjusted P-value <0.05) in cultured vs. GC B-cells. The expression profile of MMR and BER pathway genes, and genes selected for their association with CSR, SHM, and/or GCs is shown in Fig. 5. Many genes associated with SHM (*aicda, bcl6, msh6, rev1, polh, apex2*) are expressed at higher levels in GC B-cells, as are several DNA repair genes whose role is less clear (*neil1 and 3, mbd4*, *mdm2*). Several genes known to promote CSR are expressed at higher levels in cultured B cells (*apex1*, the de-ubiquitinase *usp22* (53) and the transcription factor *batf* (54). The increased ratio of APE2:APE1 expression in GC cells is seen here as a combination of increased APE2 and decreased APE1 relative to cultured B cells. The entire data set can be accessed at https://doi.org/10.5281/zenodo.7617207

In conclusion, the results support and extend our previous finding that APE1 and APE2 work together for optimal CSR (35). Furthermore, when APE1 is limiting as in the GC, repair by APE2 becomes error-prone, likely due to its inefficient AP-endonuclease activity and possible interaction with PCNA and TLPs. APE2 promotes V-region SHM and GLSμ mutations, while APE1 promotes DNA breaks but suppresses SHM in vitro. The APE2 C-terminus is required for its role in CSR but not SHM, although the impact of its interaction with PCNA merits further study.

Discussion

Historically, SHM of the J_{H4} intronic region has been undetectable in B cells activated in vitro (16–19), but has never been examined in cells with reduced APE1. We genetically modified splenic B cells to mimic the low APE1 and high APE2 expression seen in the GC and can now detect AID-dependent SHM in primary cultured B cells. Our findings demonstrate the importance of the ratio of APE1:APE2 expression levels for both SHM and CSR. Both processes have long been associated with the GC, however, it was recently shown that CSR activity declines in the GC (36), where APE1 expression is very low. APE1 creates DSBs required for CSR, but DSBs are not an intermediate during SHM. InDels that can result from DNA breaks are abundant in the non-coding switch (S) regions in cells undergoing CSR, while SHM is limited primarily to point mutations, where InDels in the Ig coding region would be deleterious to function. APE1 is not required for SHM in cell line models (55), and haploinsufficiency has no effect on SHM in vivo (1), although it does reduce CSR (35, 56). In the GC, low APE1 expression would limit the deleterious effects of DNA breaks, while increased APE2 expression promotes SHM (1) and supports B cell viability (2).

APE2 seems uniquely suited for error-prone repair. Its catalytic site is more open, able to accommodate insertion of a mispaired base (26). Also, APE2's inefficient endonuclease activity, relative to APE1, would leave more abasic sites unrepaired, causing transition and transversion mutations at the G:C bp attacked by AID. Furthermore, APE2's C-terminus can interact functionally with PCNA (27, 28), which increases its exonuclease activity, while also interacting with error-prone TLPs and MMR (30–34) that promote SHM. In the presence of PCNA, the exonuclease activity of both APE2 and MMR-associated EXO1 are more processive, so a larger gap can be excised and filled in by error-prone TLPs like Pol η, Pol ζ and REV1.

Based on our findings, we propose here a model incorporating how changes in APE1 and APE2 expression during B cell activation might shift the balance from accurate to error prone repair, and how APE1 and APE2 might work together to promote CSR. First, in a resting B cell, APE1 predominates, and its interaction with XRCC1 promotes accurate repair by Pol β and Ligase (Fig. 6A). Then, during early activation (pre-GC) when both are expressed, APE1 and APE2 work together to turn multiple AP sites into DSBs for CSR. If APE1 and APE2 cleave two AP sites on opposite strands in very close proximity, CSR independent of MMR can be explained by the 3' to 5' exonuclease activity of APE2. When stimulated by PCNA, APE2 can excise ~10-12 nucleotides (28), and could encounter a nick made by APE1 on the opposite strand, forming a DSB (Fig. 6B). If AID lesions are farther

apart, MMR is required (11). In this scenario, APE2 interacts with MMR via PCNA, and 5' to 3' strand excision by MMR-EXO1 results in DSB formation when a nick on the opposite strand is encountered (Fig. 6C). CSR in Msh2-deficient cells is reduced by 2-fold, as are GLSμ DSBs (10, 11, 57). These two models are similar in requiring exonuclease activity and are not exclusive. The distance and strand orientation between AP sites could dictate which exonuclease is used to create a DSB, since PCNA stimulates the processivity of both MMR-EXO1 and APE2-exonuclease. We tested the idea of partial redundancy between APE2 and MMR by generating DBL mice that are also deficient in MSH2. Indeed, the decrease in CSR in MSH2− and APE2-deficient B cells is additive, with CSR reduced between 3- and 6.5-fold in DBL/MSH2-deficient cells (Supplementary Fig. 5). Although APE1 likely makes more SSBs due to its efficient endonuclease activity and ability to interact with AID (58), the nicks made by APE2 might be more likely to undergo excision, contributing to DSB formation. Recent reports describe direct interaction between APE1 and APE2 during SSB repair, and a role for APE2 in SSB end resection (29, 59–61).

Finally, with rapid cell division, APE1 expression is diminished and APE2 predominates in the GC (Fig. 6D). In our model, a complex containing UNG, APE2 and PCNA recruits TLPs and MMR during G1 phase when AID is active (11, 15, 62, 63) and when non-canonical MMR can be error-prone (64). Like APE2, UNG also has a canonical PCNA-interacting domain. APE2 may also be responsible for making the nicks in DNA that permit entry of MMR and EXO1. Consistent with this, there is a 2-fold reduction in SHM in PP GC cells and a significant reduction in spreading of mutations beyond AID hotspots in *apex2*$^{Y/-}$ mice (1). The decrease is not dramatic, but redundancy in the ability of APE2, UNG and MMR to all interact with PCNA likely reduces the impact of APE2 deficiency. Indeed, there is a surprising, additive effect of combined UNG- and APE2-deficiency on SHM in the GC, where A:T mutations are further decreased compared to the single mutants (1). This was not expected since UNG acts upstream in the same pathway as APE2, but it is consistent with some redundant function such as PCNA-recruitment.

Although we did not directly demonstrate APE2-PCNA-MMR interaction in our system, we base our models on previously published functional interactions of these proteins. In addition to PCNA, the C-terminal Zf-GRF domain of APE2 has been shown to interact functionally with ATR and Chk1 to promote SSB repair (29). This function of APE2 is essential for survival of BRCA2-deficient cells (65) but is unlikely to be beneficial to CSR or SHM. Disruption of ATR/Chk1 activation would result in delayed SSB repair, which would be beneficial to both CSR and SHM, and these proteins are suppressed by BCL6 in the GC (66, 67). Indeed, CSR was slightly, though not significantly increased in B cells expressing APE2-ΔE (Fig. 4C and Supplementary Fig. 1C), which lacks the Zf-GRF domain associated with ATR/Chk1 activation.

We also modeled how SSB repair in the GC is repressed through a multi-faceted approach (Fig. 7), where (1) low APE1 expression in the GC reduces XRCC1/POLB/Ligase-mediated accurate repair of AP sites made by AID and UNG, and (2) APE2 expression is increased, but its potential to interact with ATR and Chk1 is inhibited because these proteins are suppressed by BCL6. This leaves APE2 able to promote error-prone repair through (a) its inefficient AP endonuclease activity, (b) its interaction with PCNA and associated TLPs,

and (c) its enhanced exonuclease activity stimulated by PCNA. Furthermore, with APE1 levels limiting in the GC, survival of these rapidly proliferating B cells is highly dependent upon APE2, for the repair of both AID-dependent damage and AID-independent oxidative damage (2).

In contrast, cultured B cells express APE1 and proliferate normally in the absence of APE2 (35). APE2 can promote mutations in vitro when APE1 expression is reduced, but the mutation frequency we observe at J_{H4} in culture is very low compared to that of GC B cells; too low to permit analysis of the mutation spectrum. A likely reason for the low mutation frequency in culture is that we cannot eliminate APE1, and residual APE1 levels in DBL (*apex1*$^{+/-}$) cells are sufficient to compete with APE2 to promote accurate repair of some AID lesions. Furthermore, recent studies clearly showed that AID associates poorly with V genes in cultured B cells and B cell lines relative to GC B cells, and relative to its association with Sμ (17, 18). Maul, et al. showed that the accumulation of the phosphorylated, initiating form of Pol II (Ser5P), and SpT5 with which it associates, strongly correlates with AID binding and hypermutation (17, 18, 68). Using ex vivo activated B1-8 B cells, they found that this complex accumulates at V genes and S regions in GC B cells, but only at S regions and *not* at V genes in vitro. Consistent with this, the mutation frequency was even lower in the B1-8 VDJ exon in our system, which we further showed have increased APE1 expression levels relative to B6 mice. Finally, we also found that several other genes involved in SHM are expressed at higher levels in the GC than in ex vivo B cells activated in our system. Despite the low mutation frequency, our data clearly show that AID does have activity on the J_{H4} V region in culture, but that most of these mutations are repaired accurately.

Similar to APE1, POLB mRNA expression is very low in GC B cells, and slightly higher in culture. Interestingly, expression of the essential gene XRCC1, which coordinates interaction of APE1 and POLB, is highly increased in the GC (Fig. 5) and could promote survival where the essential proteins APE1 and POLB are limiting. Previous experiments that attempted to block the APE1/XRCC1/POLB axis in cultured B cells found that CSR was slightly increased in the absence of POLB, and in B cells that are haploinsufficient for XRCC1 (*xrcc1*$^{+/}$) (69–71). To explain error-prone repair, it was suggested the POLB pathway is “overwhelmed” by too many AID-induced lesions (71), but perhaps instead it is out-competed by high levels of APE2 that recruit PCNA/TLPs instead of POLB. Similar to our results with APE1, it was recently shown that expression of POLB is very low in the GC and suppression of POLB in CH12-F3 cells results in increased GLSμ A:T mutations (5).

Interestingly, like UNG, APE2 has been shown to prefer ss DNA (29), the required template of AID. The excision of abasic sites in ss DNA by APE2 would readily promote DSB formation and CSR, even without MMR. The ss-DNA binding Zf-GRF domain was not necessary for CSR or SHM in our assays, but it would be interesting to test its importance in MMR-deficient cells. Such a pathway would likely generate substantial genomic instability and therefore merits further investigation.

Supplementary Material

Refer to Web version on PubMed Central for supplementary material.

Acknowledgements.

The authors thank the UMass Medical School Flow Cytometry Core Facility for expert cell sorting, and Drs. T. Honjo, T. Lindahl, D. Barnes, T. Mak, and E. Friedberg for mice. We thank Drs. Frederick Alt and Chong Wang for providing B1-8 mice and preliminary data on B1-8 SHM in culture, and Drs. V. Barretto, M. Nussenzweig and J. Chaudhuri for retroviral constructs. We thank Drs. J. Stavnezer, R. Woodland and J. Guikema for helpful discussions.

This work was supported by National Institutes of Health AI126122, AI023283, and AI099988 (to C.E.S.), and SBIR Phase II grant 2R44HG008917 (to BioSpyder Technologies).

Abbreviations used in this article:

AID	activation induced cytidine deaminase
APE	apurinic/apyrimidinic endonuclease
CSR	class switch recombination
DBL	*ape1*$^{+/-}$/*ape2*$^{Y/-}$ mice
DSB	double-strand break
Pol	polymerase
SHM	somatic hypermutation
SSB	single-strand break
TLP	translesion polymerase
UNG	uracil DNA glycosylase.

References

1. Stavnezer J, Linehan EK, Thompson MR, Habboub G, Ucher AJ, Kadungure T, Tsuchimoto D, Nakabeppu Y, and Schrader CE. 2014. Differential expression of APE1 and APE2 in germinal centers promotes error-prone repair and A:T mutations during somatic hypermutation. Proc Natl Acad Sci U S A 111: 9217–9222. [PubMed: 24927551]
2. Guikema JEJ, L. E. K, Esa N, Tsuchimoto D, Nakabeppu Y, Woodland RT, and Schrader CE 2014. AP endonuclease 2 regulates the expansion of germinal centers by protecting against AID-independent DNA damage in B cells. . J Immunol 193: 931–939. [PubMed: 24935922]
3. Petersen-Mahrt SK, Harris RS, and Neuberger MS. 2002. AID mutates E. coli suggesting a DNA deamination mechanism for antibody diversification. Nature 418: 99–104. [PubMed: 12097915]
4. Victora GD, and Nussenzweig MC. 2012. Germinal centers. Annu Rev Immunol 30: 429–457. [PubMed: 22224772]
5. Stratigopoulou M, van Dam TP, and Guikema JEJ. 2020. Base Excision Repair in the Immune System: Small DNA Lesions With Big Consequences. Front Immunol 11: 1084. [PubMed: 32547565]
6. Teng G, and Papavasiliou FN. 2007. Immunoglobulin somatic hypermutation. Annu Rev Genet 41: 107–120. [PubMed: 17576170]

7. Stavnezer J, Guikema JE, and Schrader CE. 2008. Mechanism and regulation of class switch recombination. Annu.Rev.Immunol 26: 261–292. [PubMed: 18370922]
8. Robbiani DF, and Nussenzweig MC. 2013. Chromosome translocation, B cell lymphoma, and activation-induced cytidine deaminase. Annual review of pathology 8: 79–103.
9. Almeida KH, and Sobol RW. 2007. A unified view of base excision repair: lesion-dependent protein complexes regulated by post-translational modification. DNA Repair (Amst) 6: 695–711. [PubMed: 17337257]
10. Stavnezer J, and Schrader CE. 2006. Mismatch repair converts AID-instigated nicks to double-strand breaks for antibody class-switch recombination. Trends Genet 22: 23–28. [PubMed: 16309779]
11. Schrader CE, Guikema JE, Linehan EK, Selsing E, and Stavnezer J. 2007. Activation-induced cytidine deaminase-dependent DNA breaks in class switch recombination occur during G1 phase of the cell cycle and depend upon mismatch repair. J Immunol 179: 6064–6071. [PubMed: 17947680]
12. Rada C, Ehrenstein MR, Neuberger MS, and Milstein C. 1998. Hot spot focusing of somatic hypermutation in MSH2-deficient mice suggests two stages of mutational targeting. Immunity 9: 135–141. [PubMed: 9697843]
13. Phung QH, Winter DB, Cranston A, Tarone RE, Bohr VA, Fishel R, and Gearhart PJ. 1998. Increased hypermutation at G and C nucleotides in immunoglobulin variable genes from mice deficient in the MSH2 mismatch repair protein. J. Exp. Med 187: 1745–1751. [PubMed: 9607916]
14. Bregenhorn S, Kallenberger L, Artola-Boran M, Pena-Diaz J, and Jiricny J. 2016. Non-canonical uracil processing in DNA gives rise to double-strand breaks and deletions: relevance to class switch recombination. Nucleic Acids Res.
15. Wang Q, Kieffer-Kwon KR, Oliveira TY, Mayer CT, Yao K, Pai J, Cao Z, Dose M, Casellas R, Jankovic M, Nussenzweig MC, and Robbiani DF. 2017. The cell cycle restricts activation-induced cytidine deaminase activity to early G1. J Exp Med 214: 49–58. [PubMed: 27998928]
16. Decker DJ, Linton PJ, Zaharevitz S, Biery M, Gingeras TR, and Klinman NR. 1995. Defining subsets of naive and memory B cells based on the ability of their progeny to somatically mutate in vitro. Immunity 2: 195–203. [PubMed: 7534621]
17. Matthews AJ, Husain S, and Chaudhuri J. 2014. Binding of AID to DNA does not correlate with mutator activity. J Immunol 193: 252–257. [PubMed: 24879790]
18. Maul RW, Cao Z, Venkataraman L, Giorgetti CA, Press JL, Denizot Y, Du H, Sen R, and Gearhart PJ. 2014. Spt5 accumulation at variable genes distinguishes somatic hypermutation in germinal center B cells from ex vivo-activated cells. J Exp Med 211: 2297–2306. [PubMed: 25288395]
19. Nojima T, Haniuda K, Moutai T, Matsudaira M, Mizokawa S, Shiratori I, Azuma T, and Kitamura D. 2011. In-vitro derived germinal centre B cells differentially generate memory B or plasma cells in vivo. Nature communications 2: 465.
20. Fung H, and Demple B. 2005. A vital role for Ape1/Ref1 protein in repairing spontaneous DNA damage in human cells. Mol Cell 17: 463–470. [PubMed: 15694346]
21. Xanthoudakis S, Smeyne RJ, Wallace JD, and Curran T. 1996. The redox/DNA repair protein, Ref-1, is essential for early embryonic development in mice. Proc Natl Acad Sci U S A 93: 8919–8923. [PubMed: 8799128]
22. Izumi T, Brown DB, Naidu CV, Bhakat KK, Macinnes MA, Saito H, Chen DJ, and Mitra S. 2005. Two essential but distinct functions of the mammalian abasic endonuclease. Proc Natl Acad Sci U S A 102: 5739–5743. [PubMed: 15824325]
23. Vidal AE, Boiteux S, Hickson ID, and Radicella JP. 2001. XRCC1 coordinates the initial and late stages of DNA abasic site repair through protein-protein interactions. EMBO J 20: 6530–6539. [PubMed: 11707423]
24. Yamamori T, DeRicco J, Naqvi A, Hoffman TA, Mattagajasingh I, Kasuno K, Jung SB, Kim CS, and Irani K. 2010. SIRT1 deacetylates APE1 and regulates cellular base excision repair. Nucleic Acids Res 38: 832–845. [PubMed: 19934257]
25. Burkovics P, Szukacsov V, Unk I, and Haracska L. 2006. Human Ape2 protein has a 3'-5' exonuclease activity that acts preferentially on mismatched base pairs. Nucleic Acids Res 34: 2508–2515. [PubMed: 16687656]

26. Hadi MZ, Ginalski K, Nguyen LH, and Wilson DM 3rd. 2002. Determinants in nuclease specificity of Ape1 and Ape2, human homologues of Escherichia coli exonuclease III. J Mol Biol 316: 853–866. [PubMed: 11866537]
27. Tsuchimoto D, Sakai Y, Sakumi K, Nishioka K, Sasaki M, Fujiwara T, and Nakabeppu Y. 2001. Human APE2 protein is mostly localized in the nuclei and to some extent in the mitochondria, while nuclear APE2 is partly associated with proliferating cell nuclear antigen. Nucleic Acids Res 29: 2349–2360. [PubMed: 11376153]
28. Burkovics P, Hajdu I, Szukacsov V, Unk I, and Haracska L. 2009. Role of PCNA-dependent stimulation of 3'-phosphodiesterase and 3'-5' exonuclease activities of human Ape2 in repair of oxidative DNA damage. Nucleic Acids Res 37: 4247–4255. [PubMed: 19443450]
29. Wallace BD, Berman Z, Mueller GA, Lin Y, Chang T, Andres SN, Wojtaszek JL, DeRose EF, Appel CD, London RE, Yan S, and Williams RS. 2017. APE2 Zf-GRF facilitates 3'-5' resection of DNA damage following oxidative stress. Proc Natl Acad Sci U S A 114: 304–309. [PubMed: 28028224]
30. Chen X, Paudyal SC, Chin RI, and You Z. 2013. PCNA promotes processive DNA end resection by Exo1. Nucleic Acids Res 41: 9325–9338. [PubMed: 23939618]
31. Masih PJ, Kunnev D, and Melendy T. 2008. Mismatch Repair proteins are recruited to replicating DNA through interaction with Proliferating Cell Nuclear Antigen (PCNA). Nucleic Acids Res 36: 67–75. [PubMed: 17984070]
32. Garg P, and Burgers PM. 2005. Ubiquitinated proliferating cell nuclear antigen activates translesion DNA polymerases eta and REV1. Proc Natl Acad Sci U S A 102: 18361–18366. [PubMed: 16344468]
33. Kannouche PL, Wing J, and Lehmann AR. 2004. Interaction of human DNA polymerase eta with monoubiquitinated PCNA: a possible mechanism for the polymerase switch in response to DNA damage. Mol Cell 14: 491–500. [PubMed: 15149598]
34. Zlatanou A, Despras E, Braz-Petta T, Boubakour-Azzouz I, Pouvelle C, Stewart GS, Nakajima S, Yasui A, Ishchenko AA, and Kannouche PL. 2011. The hMsh2-hMsh6 complex acts in concert with monoubiquitinated PCNA and Pol eta in response to oxidative DNA damage in human cells. Mol Cell 43: 649–662. [PubMed: 21855803]
35. Guikema JE, Linehan EK, Tsuchimoto D, Nakabeppu Y, Strauss PR, Stavnezer J, and Schrader CE. 2007. APE1− and APE2-dependent DNA breaks in immunoglobulin class switch recombination. J Exp Med 204: 3017–3026. [PubMed: 18025127]
36. Roco JA, Mesin L, Binder SC, Nefzger C, Gonzalez-Figueroa P, Canete PF, Ellyard J, Shen Q, Robert PA, Cappello J, Vohra H, Zhang Y, Nowosad CR, Schiepers A, Corcoran LM, Toellner KM, Polo JM, Meyer-Hermann M, Victora GD, and Vinuesa CG. 2019. Class-Switch Recombination Occurs Infrequently in Germinal Centers. Immunity 51: 337–350 e337. [PubMed: 31375460]
37. Sabouri Z, Okazaki IM, Shinkura R, Begum N, Nagaoka H, Tsuchimoto D, Nakabeppu Y, and Honjo T. 2009. Apex2 is required for efficient somatic hypermutation but not for class switch recombination of immunoglobulin genes. Int Immunol 21: 947–955. [PubMed: 19556307]
38. Meira LB, Devaraj S, Kisby GE, Burns DK, Daniel RL, Hammer RE, Grundy S, Jialal I, and Friedberg EC. 2001. Heterozygosity for the mouse Apex gene results in phenotypes associated with oxidative stress. Cancer Res 61: 5552–5557. [PubMed: 11454706]
39. Ide Y, Tsuchimoto D, Tominaga Y, Nakashima M, Watanabe T, Sakumi K, Ohno M, and Nakabeppu Y. 2004. Growth retardation and dyslymphopoiesis accompanied by G2/M arrest in APEX2-null mice. Blood 104: 4097–4103. [PubMed: 15319281]
40. Shih TA, Roederer M, and Nussenzweig MC. 2002. Role of antigen receptor affinity in T cell-independent antibody responses in vivo. Nat Immunol 3: 399–406. [PubMed: 11896394]
41. Barreto V, Reina-San-Martin B, Ramiro AR, McBride KM, and Nussenzweig MC. 2003. C-terminal deletion of AID uncouples class switch recombination from somatic hypermutation and gene conversion. Mol Cell 12: 501–508. [PubMed: 14536088]
42. Ranjit S, Khair L, Linehan EK, Ucher AJ, Chakrabarti M, Schrader CE, and Stavnezer J. 2011. AID binds cooperatively with UNG and Msh2-Msh6 to Ig switch regions dependent upon the AID C terminus. J. Immunol 187: 2464–2475. [PubMed: 21804017]

43. Vuong BQ, Lee M, Kabir S, Irimia C, Macchiarulo S, McKnight GS, and Chaudhuri J. 2009. Specific recruitment of protein kinase A to the immunoglobulin locus regulates class-switch recombination. Nat Immunol 10: 420–426. [PubMed: 19234474]
44. McDonald JP, Frank EG, Plosky BS, Rogozin IB, Masutani C, Hanaoka F, Woodgate R, and Gearhart PJ. 2003. 129-derived strains of mice are deficient in DNA polymerase i and have normal immunoglobulin hypermutation. J. Exp. Med 198: 635–643. [PubMed: 12925679]
45. Schrader CE, Bradley SP, Vardo J, Mochegova SN, Flanagan E, and Stavnezer J. 2003. Mutations occur in the Ig Smu region but rarely in Sgamma regions prior to class switch recombination. EMBO J. 22: 5893–5903. [PubMed: 14592986]
46. Schrader CE, Bradley SP, Vardo J, Mochegova SN, Flanagan E, and Stavnezer J. 2003. Mutations occur in the Ig Sμ region but rarely in Sγ regions prior to class switch recombination. Embo J 22: 5893–5903. [PubMed: 14592986]
47. Xue K, Rada C, and Neuberger MS. 2006. The in vivo pattern of AID targeting to immunoglobulin switch regions deduced from mutation spectra in msh2−/− ung−/− mice. J Exp Med 203: 2085–2094. [PubMed: 16894013]
48. Love MI, Huber W, and Anders S. 2014. Moderated estimation of fold change and dispersion for RNA-seq data with DESeq2. Genome Biol 15: 550. [PubMed: 25516281]
49. Yeakley JM, Shepard PJ, Goyena DE, VanSteenhouse HC, McComb JD, and Seligmann BE. 2017. A trichostatin A expression signature identified by TempO-Seq targeted whole transcriptome profiling. PloS one 12: e0178302. [PubMed: 28542535]
50. Li H, Qiu J, and Fu XD. 2012. RASL-seq for massively parallel and quantitative analysis of gene expression. Curr Protoc Mol Biol Chapter 4: Unit 4 13 11–19.
51. Yeakley JM, Fan JB, Doucet D, Luo L, Wickham E, Ye Z, Chee MS, and Fu XD. 2002. Profiling alternative splicing on fiber-optic arrays. Nat Biotechnol 20: 353–358. [PubMed: 11923840]
52. Trejo CL, Babic M, Imler E, Gonzalez M, Bibikov SI, Shepard PJ, VanSteenhouse HC, Yeakley JM, and Seligmann BE. 2019. Extraction-free whole transcriptome gene expression analysis of FFPE sections and histology-directed subareas of tissue. PLoS One 14: e0212031. [PubMed: 30794557]
53. Li C, Irrazabal T, So CC, Berru M, Du L, Lam E, Ling AK, Gommerman JL, Pan-Hammarstrom Q, and Martin A. 2018. The H2B deubiquitinase Usp22 promotes antibody class switch recombination by facilitating non-homologous end joining. Nature communications 9: 1006.
54. Ise W, Kohyama M, Schraml BU, Zhang T, Schwer B, Basu U, Alt FW, Tang J, Oltz EM, Murphy TL, and Murphy KM. 2011. The transcription factor BATF controls the global regulators of class-switch recombination in both B cells and T cells. Nat Immunol 12: 536–543. [PubMed: 21572431]
55. Islam H, Kobayashi M, and Honjo T. 2019. Apurinic/apyrimidinic endonuclease 1 (APE1) is dispensable for activation-induced cytidine deaminase (AID)-dependent somatic hypermutation in the immunoglobulin gene. Int Immunol 31: 543–554. [PubMed: 30877298]
56. Masani S, Han L, and Yu K. 2013. Apurinic/apyrimidinic endonuclease 1 is the essential nuclease during immunoglobulin class switch recombination. Mol Cell Biol 33: 1468–1473. [PubMed: 23382073]
57. Schrader CE, Edelmann W, Kucherlapati R, and Stavnezer J. 1999. Reduced isotype switching in splenic B cells from mice deficient in mismatch repair enzymes. J. Exp. Med 190: 323–330. [PubMed: 10430621]
58. Vuong BQ, Herrick-Reynolds K, Vaidyanathan B, Pucella JN, Ucher AJ, Donghia NM, Gu X, Nicolas L, Nowak U, Rahman N, Strout MP, Mills KD, Stavnezer J, and Chaudhuri J. 2013. A DNA break- and phosphorylation-dependent positive feedback loop promotes immunoglobulin class-switch recombination. Nat Immunol 14: 1183–1189. [PubMed: 24097111]
59. Lin Y, Raj J, Li J, Ha A, Hossain MA, Richardson C, Mukherjee P, and Yan S. 2020. APE1 senses DNA single-strand breaks for repair and signaling. Nucleic Acids Res 48: 1925–1940. [PubMed: 31828326]
60. Hossain MA, Lin Y, and Yan S. 2018. Single-Strand Break End Resection in Genome Integrity: Mechanism and Regulation by APE2. Int J Mol Sci 19.

61. Alvarez-Quilon A, Wojtaszek JL, Mathieu MC, Patel T, Appel CD, Hustedt N, Rossi SE, Wallace BD, Setiaputra D, Adam S, Ohashi Y, Melo H, Cho T, Gervais C, Munoz IM, Grazzini E, Young JTF, Rouse J, Zinda M, Williams RS, and Durocher D. 2020. Endogenous DNA 3' Blocks Are Vulnerabilities for BRCA1 and BRCA2 Deficiency and Are Reversed by the APE2 Nuclease. Mol Cell 78: 1152–1165 e1158. [PubMed: 32516598]

62. Le Q, and Maizels N. 2015. Cell Cycle Regulates Nuclear Stability of AID and Determines the Cellular Response to AID. PLoS genetics 11: e1005411. [PubMed: 26355458]

63. Sharbeen G, Yee CW, Smith AL, and Jolly CJ. 2012. Ectopic restriction of DNA repair reveals that UNG2 excises AID-induced uracils predominantly or exclusively during G1 phase. J Exp Med 209: 965–974. [PubMed: 22529268]

64. Pena-Diaz J, Bregenhorn S, Ghodgaonkar M, Follonier C, Artola-Boran M, Castor D, Lopes M, Sartori AA, and Jiricny J. 2012. Noncanonical mismatch repair as a source of genomic instability in human cells. Mol Cell 47: 669–680. [PubMed: 22864113]

65. Mengwasser KE, Adeyemi RO, Leng Y, Choi MY, Clairmont C, D'Andrea AD, and Elledge SJ. 2019. Genetic Screens Reveal FEN1 and APEX2 as BRCA2 Synthetic Lethal Targets. Mol Cell 73: 885–899 e886. [PubMed: 30686591]

66. Ranuncolo SM, Polo JM, Dierov J, Singer M, Kuo T, Greally J, Green R, Carroll M, and Melnick A. 2007. Bcl-6 mediates the germinal center B cell phenotype and lymphomagenesis through transcriptional repression of the DNA-damage sensor ATR. Nat Immunol 8: 705–714. [PubMed: 17558410]

67. Ranuncolo SM, Polo JM, and Melnick A. 2008. BCL6 represses CHEK1 and suppresses DNA damage pathways in normal and malignant B-cells. Blood cells, molecules & diseases 41: 95–99.

68. Pavri R, Gazumyan A, Jankovic M, Di Virgilio M, Klein I, Ansarah-Sobrinho C, Resch W, Yamane A, Reina San-Martin B, Barreto V, Nieland TJ, Root DE, Casellas R, and Nussenzweig MC. 2010. Activation-induced cytidine deaminase targets DNA at sites of RNA polymerase II stalling by interaction with Spt5. Cell 143: 122–133. [PubMed: 20887897]

69. Saribasak H, Maul RW, Cao Z, McClure RL, Yang W, McNeill DR, Wilson DM 3rd, and Gearhart PJ. 2011. XRCC1 suppresses somatic hypermutation and promotes alternative nonhomologous end joining in Igh genes. J Exp Med 208: 2209–2216. [PubMed: 21967769]

70. Han L, Mao W, and Yu K. 2012. X-ray repair cross-complementing protein 1 (XRCC1) deficiency enhances class switch recombination and is permissive for alternative end joining. Proc Natl Acad Sci U S A 109: 4604–4608. [PubMed: 22392994]

71. Wu X, and Stavnezer J. 2007. DNA polymerase beta is able to repair breaks in switch regions and plays an inhibitory role during immunoglobulin class switch recombination. J Exp Med 204: 1677–1689. [PubMed: 17591858]

Key Points

- High expression of APE1 and APE2 early after activation promote CSR
- After initial activation, APE1 protein dilutes out with cell division
- APE2 remains highly expressed and promotes SHM that is suppressed by APE1

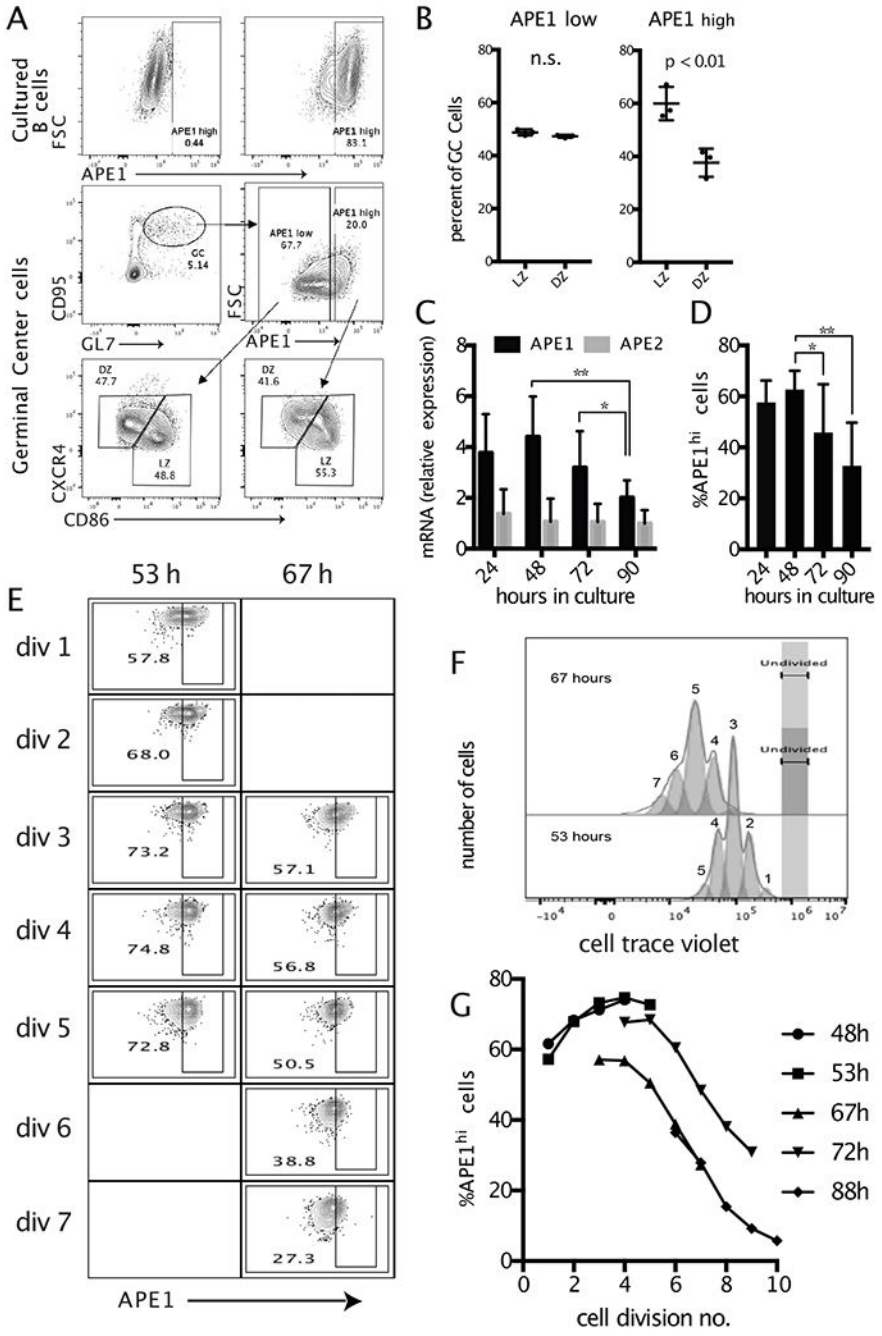

Figure 1. APE1 expression is low in GC and decreases with cell division in cultured B cells.

(A) Flow cytometric analysis of APE1 by intracellular staining in 48 hr activated spleen B cells (top row; left panel is no-first step staining control) and PP GC cells (middle row); GC APE1^{lo} and APE1^{hi} gated cells analyzed for LZ and DZ markers (bottom row). **(B)** Quantification of LZ/DZ analysis as in (A), n = 3. T-test of significance is shown. Analysis of **(C)** APE1 and APE2 mRNA by RT-PCR, relative to 18S and **(D)** APE1 protein by flow cytometry, over time in cultured B cells. APE1 protein by cell division **(E)** in cells stained

with Cell Trace Violet **(F)** cultured for 53 or 67 hr, as indicated. **(G)** Quantification of APE1 per cell division in cells harvested at the time points indicated after activation.

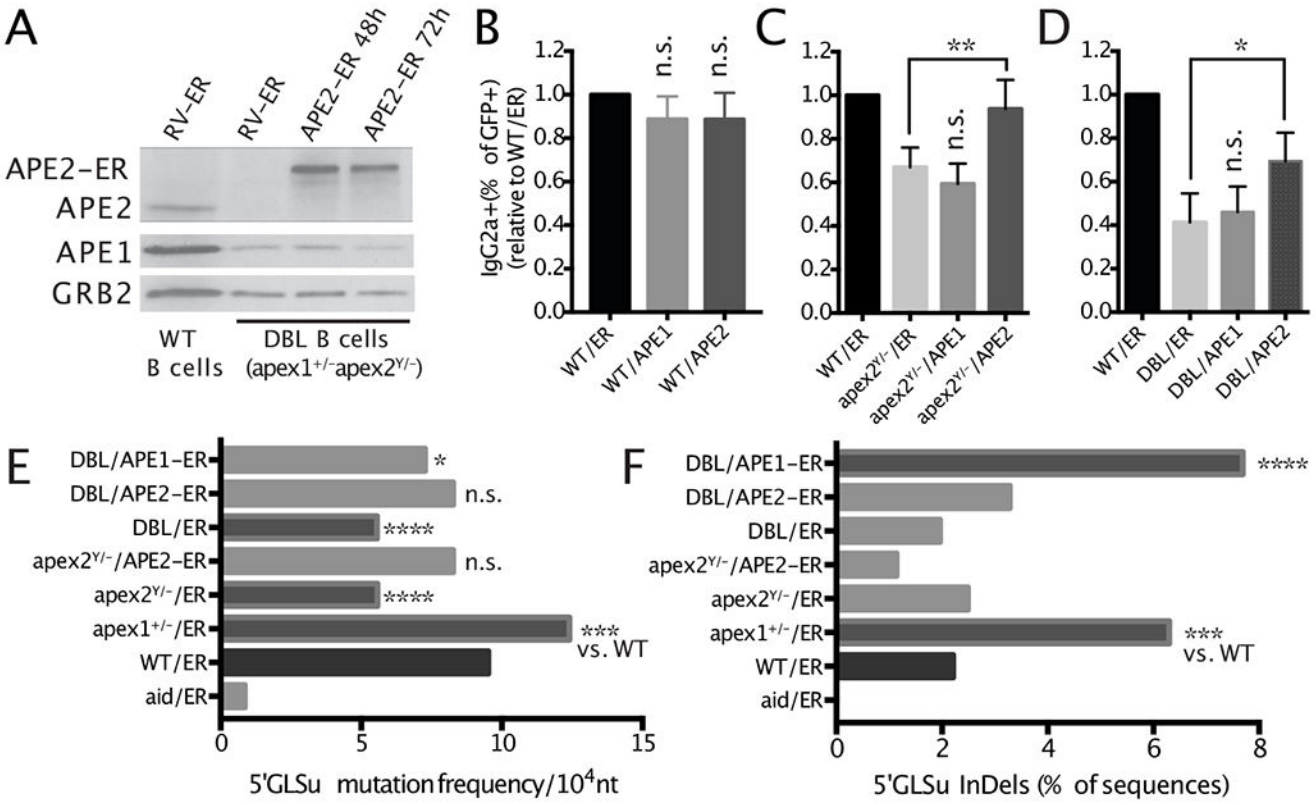

Figure 2. APE1 and APE2 both promote CSR while APE2 promotes mutations in germline Sμ.

CSR in cultures with altered APE levels. (**A**) Western blot of 20 ug WCE from WT or DBL B cells infected with RV, as indicated. Anti-APE2 antibody detects both endogenous and ER-tagged APE2. RV-ER control samples from 48 h cultures, others as indicated. (**B – D**) CSR to IgG2a on day 3 (2 days post-RV infection) relative to WT/ER control. B cell genotype/RV as indicated: e.g., *apex2*$^{Y/-}$/APE2-ER. DBL is *apex1*$^{+/-}$*apex2*$^{Y/-}$. Average of 3 independent experiments shows IgG2a+ cells as percent of GFP+ cells, relative to WT/ER control. (**C, D**) RV-APE2, but not RV-APE1, restores or increases CSR relative to vector controls (*apex2*$^{Y/-}$/ER and DBL/ER, respectively) (T-test, * $p < 0.05$, ** $p < 0.01$). (**E**) Mutations, including InDels, per 10^3 bp, in GFP+ IgM+ FACS-purified B cells after 5 days in culture (4 days post-RV infection). (**F**) Percent of GLSμ sequences with insertion/deletion mutations (InDels). (**E, F**) Significance vs. WT/ER by Chi-square analysis is indicated (* $p < 0.05$, *** $p < 0.001$, **** $p < 0.0001$). Each data point is from 2 or 3 independent experiments and ranges from 95,123 to 152,796 total nt sequenced at 749 nt/sequence, except for *aid* control (n = 1, 69,657 nt sequenced). Details of data set and analysis in Supplementary Table S1.

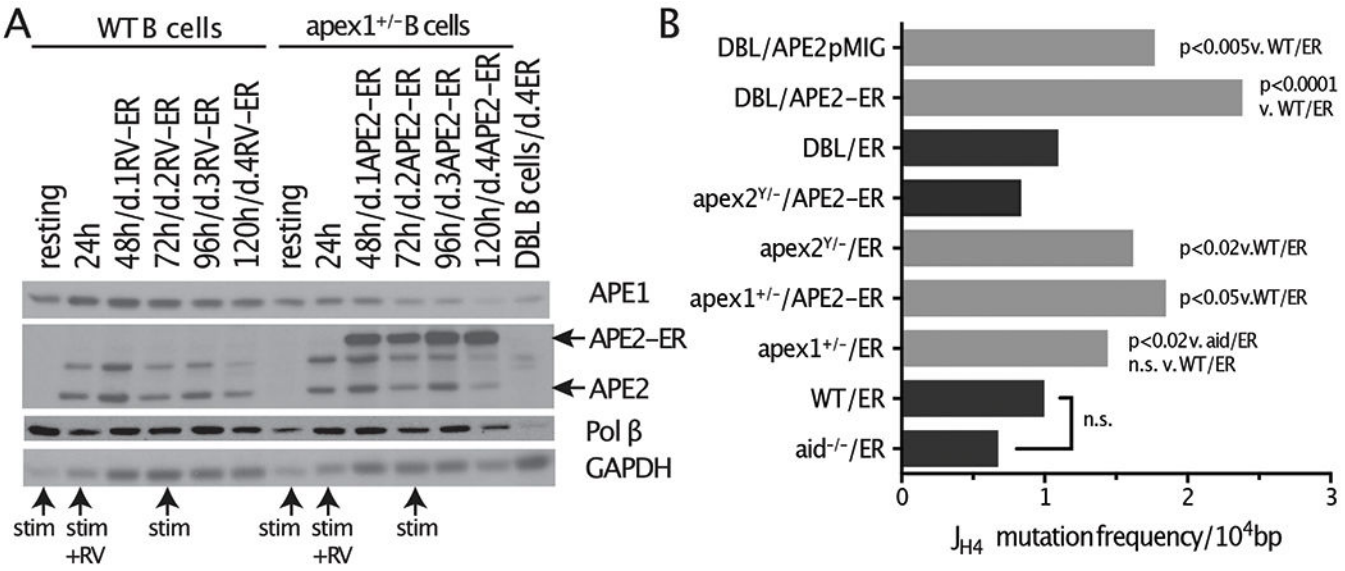

Figure 3. APE2 promotes mutations in J_{H4} intron in cultured B cells with reduced APE1 expression.

(**A**) Western blot of 20 ug WCE from WT or *apex1*$^{+/-}$ B cells infected with control RV-ER or APE2-ER, respectively, as a function of time in culture, indicated as hrs post-activation/ days post-RV infection. Timing of re-stimulation or RV-infection is indicated by arrows below. (**B**) Mutations in J_{H4} intron segment per 10^4 bp in GFP+ IgM− FACS-purified B cells after 5 days in culture (4 days post-RV infection). Each data point is from 2 to 4 independent experiments and ranges from 69,372 to 152,520 total nt sequenced at 492 nt/sequence. Details of data set and analysis in Supplementary Table S2.

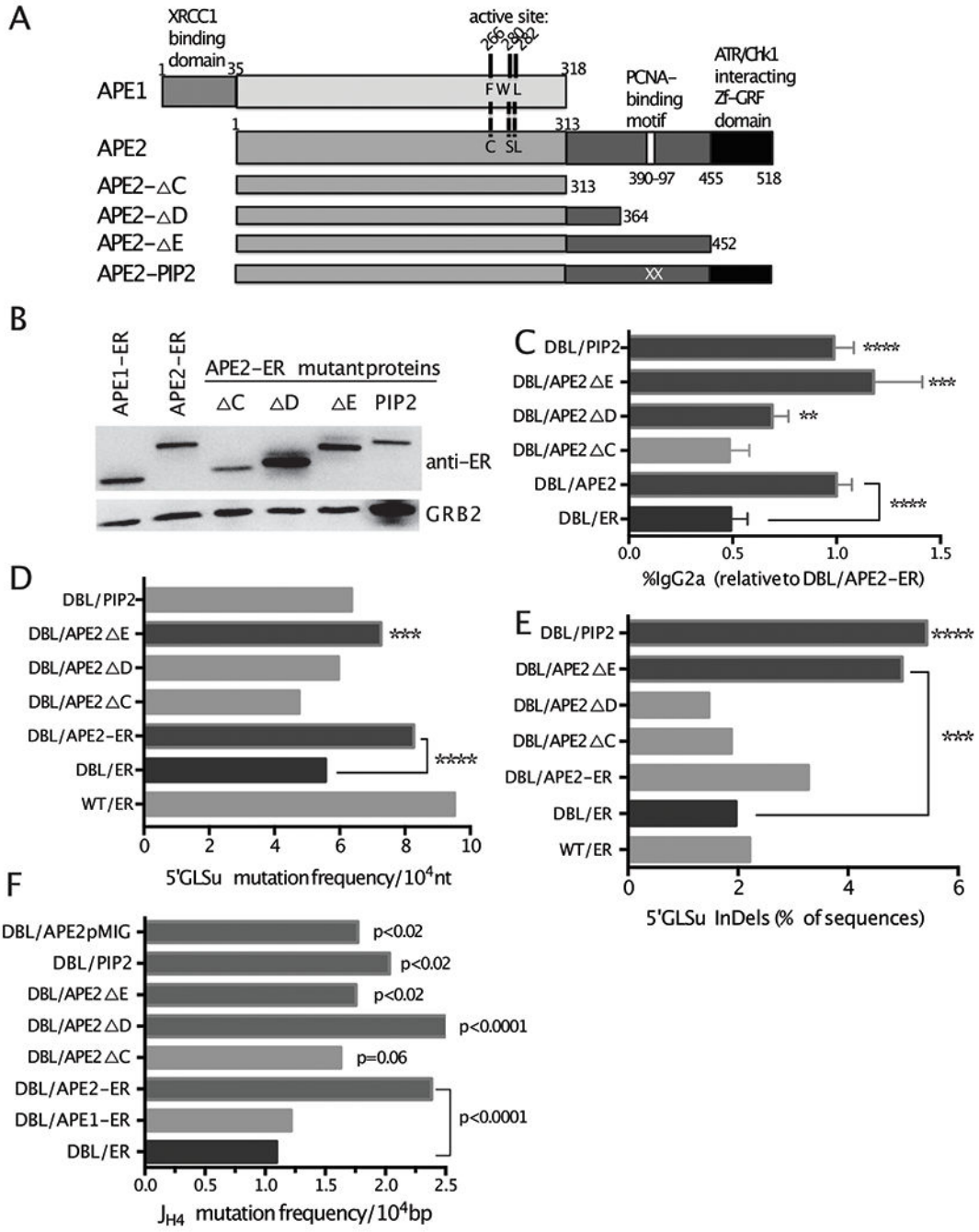

Figure 4. The APE2 C-terminus promotes mutations and CSR.

(**A**) Schematic showing conserved enzymatic core domains of APE1 and APE2 and their unique N− and C-termini, respectively. Key aa changes that affect endonuclease and exonuclease activity are shown. (**B**) Expression of APE WT and mutant ER-tagged proteins shown by western blot; 20 ug WCE, unsorted cells. The C-terminus is required to restore CSR (**C**) and GLSμ mutations (**D**) in DBL/ER cells. (**C**) n = 3 independent CSR experiments; IgG2a+ cells as percent of GFP+ cells, normalized to DBL/APE2. (**D**) Each data point is from 2 or 3 independent experiments and ranges from 101,864 to 204,477

total nt sequenced at 749 nt/sequence. Significance vs. DBL/ER indicated by T-test (**C**) and ChiSquared analysis (**D**). (**E**) Percent of GLSμ sequences with insertion/deletion mutations (InDels). (**D**, **E**) Details of data set in Suppl. Table S1. (**C, D, E**) (** $p < 0.01$, *** $p < 0.001$, **** $p < 0.0001$). (**F**) J_H4 intron mutation frequency per 10^4 bp. Each data point is from 4 to 5 independent experiments and ranges from 128,904 to 148,092 total nt sequenced, except for *DBL/PIP2* (n = 3, 73,800 nt sequenced), at 492 nt/sequence. Significance vs. DBL/ER by Chi-square analyses is shown. Details of data set in Supplementary Table S2**.**

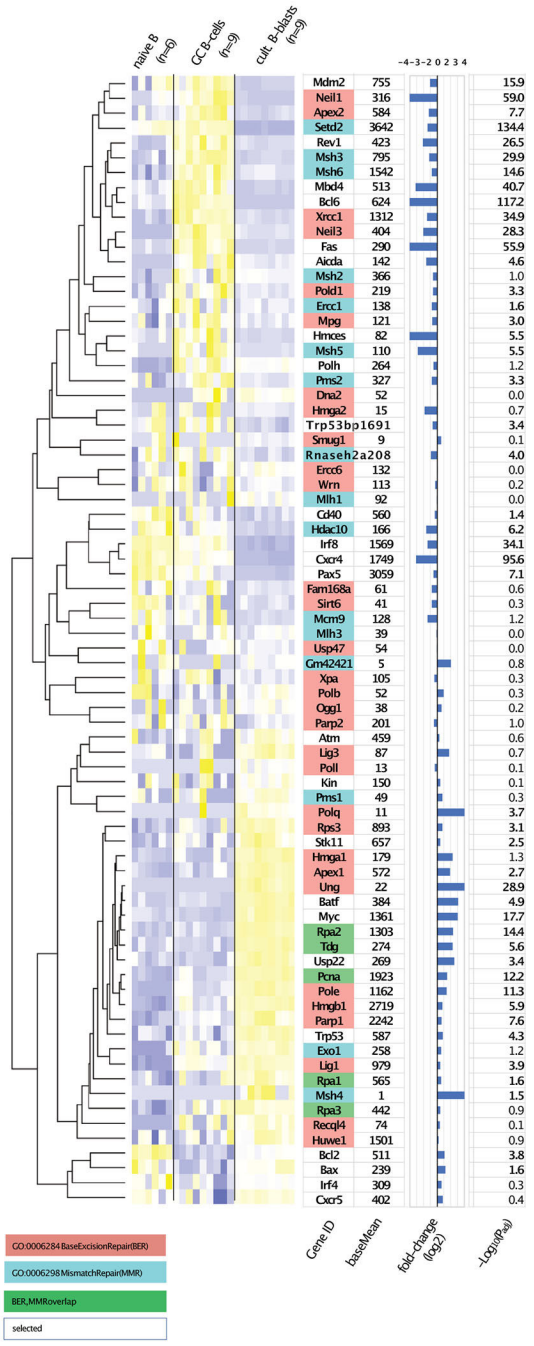

Figure 5. Relative gene expression in cultured vs. GC B cells.

Whole-genome RNA profiling of FACS-purified GC B cells (B220$^+$ CD95$^+$ GL7$^+$) and 42-hr cultured B cells (B220$^+$ GL7$^+$), (100 cells/sample; n = 9 replicates, 3 from each of 3 mice). BaseMean indicates average normalized sequence reads and reflects mRNA expression level, The Log_2-fold change chart illustrates differential expression between GC and cultured B cells, with adjusted p-values < 0.05 ((neg)Log10 > 1.3, in bold font). Follicular, naive B cells (B220$^+$ CD95$^-$ GL7$^-$; n = 6 from 2 mice) are shown for visual comparison only.

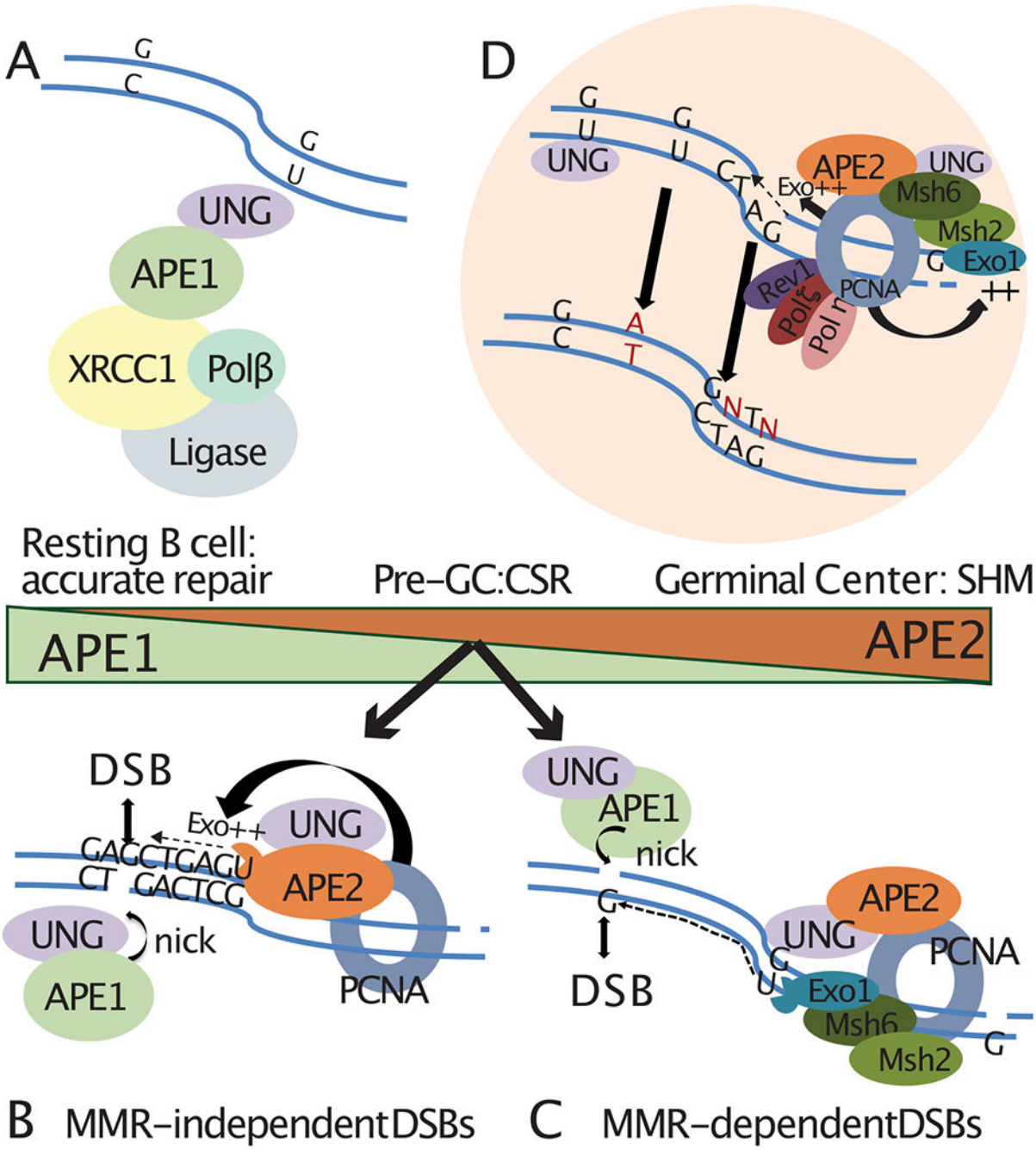

Figure 6. APE1:APE2 expression changes during B cell activation impact accurate vs. error-prone repair.

Expression levels indicated by center bar. (**A**) Accurate repair by APE1 is coordinated by XRCC1 in most cells, including resting B cells that do not express APE2. Models proposed for error-prone repair by APE2 in DSB formation during CSR (**B, C**), and in the GC (**D**). (**B, C**) APE1 and APE2 are both expressed in activated, pre-GC B-cells, and act together for optimal CSR. (**B**) MMR-independent Sμ DSBs form during CSR from AID lesions in close proximity on opposite strands. APE2 exonuclease can excise 5’ to 3’ from a nicked

AP-site to reach an AP-site nicked by APE1 on the opposite strand, forming a DSB. (**C**) MMR-dependent Sμ DSBs form when AID lesions are farther apart, promoted by interaction of APE2 with PCNA, MMR and EXO1. EXO1 3' to 5' exonuclease activity, enhanced by PCNA, can excise hundreds of nucleotides to reach a nick made by APE1 on the opposite strand. (**D**) The $APE1^{lo}$ $APE2^{hi}$ GC phenotype contributes to error-prone repair of AID lesions through APE2's inefficient endonuclease activity, interaction with PCNA that coordinates MMR and TLP activity, and exonuclease activity, enhanced by PCNA, that can excise a patch to be filled in by TLPs.

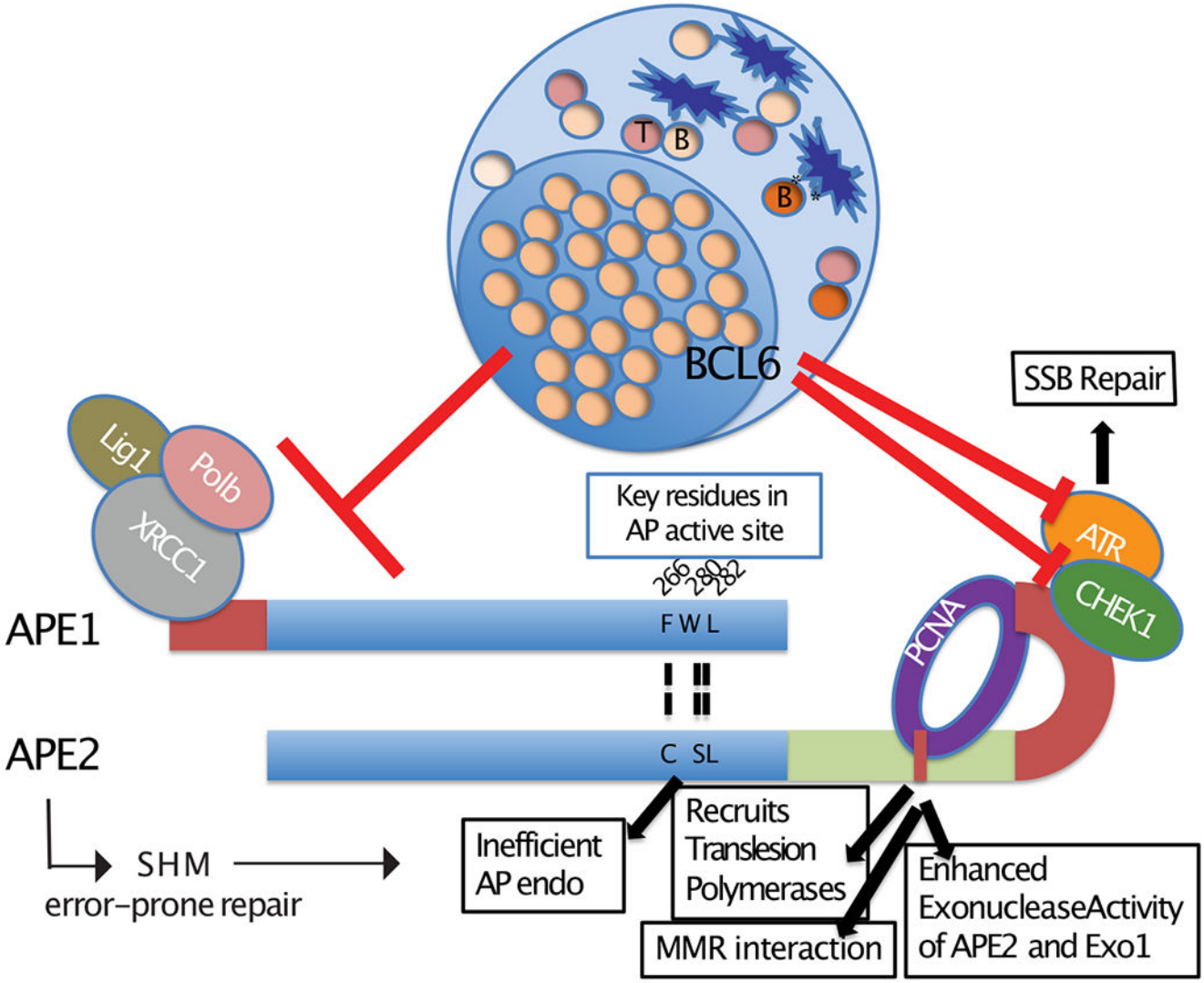

Figure 7. Suppression of accurate SSB repair in the GC includes modulation of APE1 and APE2 activity.

Decreased APE1 expression in the GC disrupts accurate SSB repair by the APE1/XRCC1/POLB/Ligase1 complex. APE2 is highly expressed, but its ability to activate the SSB response proteins ATR and Chek1 is blocked by BCL6 suppression of ATR and Chek1. APE2 promotes SHM by error-prone repair of AID/UNG lesions through mechanisms indicated and described in Fig. 6.